NUCLEAR REACTIONS OF ^{12}C, ^{20}Ne and ^{40}Ar INDUCED BY 14 MeV NEUTRONS

by

STANLEY KARDONSKY

A dissertation submitted to the Graduate faculty in Chemistry in partial fulfillment of the requirements for the degree of Doctor of Philosophy

The City University of New York

1970

This manuscript has been read and accepted for the Graduate Faculty in Chemistry in satisfaction of the dissertation requirement for the degree of Doctor of Philosophy.

2/6/70
date

Chairman of Examining Committee

2/6/70
date

Executive Officer

Supervisory Committee

The City University of New York

ACKNOWLEDGEMENTS

The author wishes to express his sincerest appreciation to the members of his advisory committee for their comments and valuable suggestions during the preparation of this dissertation. Special thanks must go to Dr. H.L. Finston and Dr. E.T. Williams for their repeated encouragement and for the forceful pushes that were sometimes necessary.

We would like to thank Mr. Dale Henderson of Argonne National Laboratory for his assistance in obtaining the gridded ionization chamber and for his advice concerning its use.

This manuscript is dedicated to the authors wife, Elaine, who put up with it all.

TABLE OF CONTENTS

LIST OF TABLES

LIST OF FIGURES

I. INTRODUCTION

Basic Reaction Theory

The term "nuclear reaction" is used to describe the results of the many processes arising from collisions of nuclei[1]. Consider the nuclei I, with Z_I protons and A_I total nucleons, to be incident on target nuclei T. These nuclei may interact by means of their nuclear forces and yield product nuclei O and P. This is symbolized

$$T + I \rightarrow O + P$$

or

$$T(I,O)P$$

In many cases I and O are neutrons, protons, or light nuclei such as alpha particles, while T and P are heavier nuclei. Typical examples of this can be seen in some of the reactions studied in this work, e.g. $^{12}C(n,\alpha)^{9}Be$ and $^{20}Ne(n,p)^{20}F$, and in reactions such as $^{12}C(d,p)^{13}C$ and $^{107}Ag(p,n)^{107}Cd$. Reactions in which I and O are heavier nuclides are also prevalent.

Other nuclear reactions which commonly occur include those which result in more than two final nuclei, or only one final nucleus. Many reactions are also induced by electromagnetic effects rather than collisions of two nuclei.

The (n,γ) reaction is an example of a nuclear reaction

in which only one product nucleus is formed. In this reaction the target nucleus absorbs the incident neutron and the resulting isotope, which is in an excited state, decays by emitting γ rays, or in some cases γ and β rays. Reactions which yield more than two product nuclei include fission, in which the target nucleus absorbs a neutron and breaks into two roughly equal fragments, and several neutrons, spallation, in which the target nucleus breaks up into fragments of unequal mass, and reactions of the type (n,2n), (n,np) and (n,2α). The problem of whether fission and the (n,2n) type reactions occur in one step, or in a series of two product reactions, is not resolved. The actual nature of the mechanism, in these cases, depends on the time in--volved as well as the theoretical frame of reference in which the reaction is to be considered.

Although not all nuclear reactions go through a compound nuclear state, in which the nucleons of the incident particle and target nucleus come within a region of nuclear dimensions for a period of time long enough to constitute a compound nucleus, it is convenient to speak of all nuclear reactions in terms of the breaking up of such a compound system. This assumption leads to a conclusion (equation 5) which is valid for all nuclear reactions regardless of their individual mechanisms. The various modes of breakup of the compound nucleus are termed reaction channels.

In the reaction T(I,O)P, T and I would constitute the entrance, or incident, channel, while O and P and all other possible products of the reaction of T and I, O' and P', would make up the various reaction channels. We, more rigorously, define a reaction channel as a possible pair consisting of product nucleus and outgoing particle, each in a definite quantum state. The specification of the channel includes the spin and orbital angular momentum orientations.

The kinetic energy in each channel is fixed by the energy of the incident channel through the equation

$$T_i - B_T - B_I + E_T^* + E_I^* = T_f - B_P - B_O + E_P^* + E_O^* \qquad (1)$$

where T_i is the kinetic energy of relative motion of T and I when they are far apart,

B is the ground state binding energy of the particle denoted by the subscript,

E^* is the energy of excitation of the particle denoted by the subscript,

and T_f is the kinetic energy of relative motion of O and P when they are far apart.

Usually E_T^* and E_I^* are zero and, very often, E_O^* is also zero. It is convenient to call the incident and final channels α and β respectively and to introduce the separation energies S_I and S_O for removing I and O from the ground state of the compound nucleus.

$$S_I = B_C - B_I - B_T$$

$$S_O = B_C - B_O - B_P$$

We then define the Q-value from channel α to channel β as the energy

$$Q_{\alpha\beta} = S_I - S_O - (E_P^* + E_O^*) + (E_T^* + E_I^*) \quad (2)$$

and the channel energies ε_α and ε_β are defined as the center of mass equivalant of the lab system energies T_i and T_f. Equation (1) can be rewritten

$$\varepsilon_\beta = \varepsilon_\alpha + Q_{\alpha\beta}. \quad (3)$$

In the absence of excitation energy in either entrance or exit channel $Q_{\alpha\beta}$ reduces to

$$Q_{IO} = S_I - S_O \quad (4)$$

Thus for a compound nucleus reaction the kinetic energy shared by the products is given by

$$\varepsilon_{OP} = T_i + Q_{IO} \quad (5)$$

Reactions in which Q_{IO} is positive are exoergic. When Q_{IO} is negative the reaction is endoergic and will not occur until T_i exceeds the threshhold energy $-Q_{IO}$.

While a positive value for ε_{OP} indicates that a reaction does occur, its magnitude provides no information as to the extent to which it will proceed. The measurable quantity that will supply such information is the nuclear cross-section, σ , which is the probability that a particular nuclear reaction will occur at a given energy.

Theoretical considerations lead to different expressions for the cross sections of reactions which proceed by compound nucleus and direct mechanisms. Comprehensive discussions of these derivations are available in various

excellent treatises on nuclear physics[1,2]. One of the most significant differences between reactions which proceed by compound state as opposed to direct mechanisms is the relation of the reaction channel to the incident channel. In a compound nucleus reaction the reaction channel will be essentially independent of the nature of the incident channel in the center of mass coordinate system with the restriction that total angular momentum is conserved. In such cases the angular distribution of the nucleon O from the T(I,O)P reaction should be isotropic in the center of mass coordinate system, since the break-up of the compound nucleus would be equally probable in any direction. Stating this in other terms: the differential cross section does not vary as the angle of observation is varied from 0^{o} to 180^{o} from the direction of the incident particle I. An example of this is the reaction $^{3}H(d,n)^{4}He$ which proceeds via the compound nucleus ^{5}He and yields an essentially isotropic flux of neutrons.

The direct reaction is a one step process. This was first recognized by Oppenheimer and Phillips[3] upon analysis of low energy (d,p) reactions[4]. It was observed experimentally that (d,p) reactions were more frequent than (d,n) reactions. This is opposite from what would be expected if the reaction had proceeded through the formation of a compound nucleus since the absence of a coulomb

barrier for expulsion of a neutron, from the compound nucleus, would lead to a preponderance of (d,n) over (d,p) reactions. Oppenheimer and Phillips explained the reaction by stating that the deuteron is a loosely bound system from which the proton is detached by the coulomb field as it approached the target nucleus. The neutron, on the other hand, is captured. This leads to an angular distribution of disintegration products peaked in the forward direction.

The theoretical confirmation for the shape of the angular distribution of direct reactions is found in the work of Butler[5-7] who showed that the angular distribution is given by the square of the spherical Bessel function of order l, where l is the orbital angular momentum of the captured nucleon.

The particular type of process of which (d,p) and (d,n) reactions are examples is called stripping. It is a single step process without the formation of a compound nucleus. At short distances, due to the strong interaction between the target nucleus and one of the two nucleons of the deuteron, either the neutron or proton is captured with the uncaptured nucleon proceeding in a forward direction. Reactions of the reverse order are called pick up reactions and can be understood in much the same manner as the above. For example, in the (n,d) reaction the incident neutron would approach the target nucleus and interact with an outer proton; these two nucleons then are

emitted as a deuteron in the direction of travel of the incident neutron. Cases in which more than one nucleon is stripped from, or picked up by, the incident particle e.g. (α,p), (n,α), (n,t) can also occur by the same mechanism, i.e. a one step process involving transfer of a group of nucleons.

There is another mechanism for direct reactions which is called heavy particle or exchange stripping. This mechanism, which contributes to an angular distribution peaked at large angles (backward), can be explained by again considering the (d,p) reaction. The target nucleus and the deuteron coalesce, except for on proton of the target which continues to move with just the momentum that it had at the time of coalescence. The process is a stripping reaction in which the roles of target and incident particle have been reversed. Many reactions whose angular distributions are peaked in the forward direction primarily, also show a certain amount of backward peaking indicating that these reactions proceed via a combination of stripping and heavy particle stripping mechanisms[8-10].

The final kinetic energy for a direct reaction is given by equation (5). It is important to note however that in a compound nucleus reaction the kinetic energy ε_{OP}, is shared among O and P while in a direct mechanism essentially all the final kinetic energy goes to particle O.

Experimental Methods

The determination of cross sections for nuclear reactions is often performed by means of techniques involving activation, in which a nuclear reaction is induced and a radioactive product nuclide is then studied. In instances where the half life of the product is convenient, its chemical separation is straightforward, and its radiations are characteristic, these techniques are very powerful and can yield highly accurate results.

In many nuclear reactions, only some, or none of the criteria listed above are met, and the use of activation analysis in determine cross sections is difficult, or even impossible. If the half life of the radioactive product is short (on the order of a few seconds or less) it would be impossible to be able to separate, and to prepare, a sample of the nuclide before its activity had disappeared. If the chemical separation is complex, time consuming, and not complete, there will be a loss in activity in separation as well as from decay. If the other products of the nuclear bombardment emit characteristic radiations which obscure those under study, verification of the desired nuclide would be difficult. Finally, if the half life is exceedingly long, or the product nuclide stable, there is no activity produced.

The limitations imposed by activation methods restricts the type of information which may be obtained. Angular distribution studies and determination of cross sections

to different energy levels are indicative of the type of information that activation cannot provide.

Many of these limitations can be avoided by studying the nuclear reaction in-situ, that is, to observe the charged particles emitted in nuclear reactions with detectors which are sensitive to such particles. It is thus possible not only to determine the overall reaction cross section but also to study angular distributions and energy levels of the compound or product nucleus.

In-situ techniques have been used extensively in the past. Schwalm and Povh[11] used surface barrier detectors to study the alpha emitting states of ^{12}C following the β decay of ^{12}B and ^{12}N. Both Bachinger and Uhl[12] and LeRoux et al[13], used nuclear emulsions to study the $^{14}N(n,\alpha)^{11}B$ reaction and, from the angular distributions obtained, concluded that the mechanism was a direct reaction. Mathur and Morgan[14] used argon filled scintillation spectrometers as well as the activation technique to study the cross section of $^{40}Ar(n,\alpha)^{37}S$ with neutrons from 13.0 to 20,2 MeV and compared their results with predictions based on the formation of a compound nucleus. S. Petralia and his co-workers used a cloud chamber to study the $^{20}Ne(n,\alpha)^{17}O$ reaction[15] and in doing so first observed the $^{20}Ne(n,2\alpha)^{13}C$ reaction[16] which apparently goes through a heavy particle stripping mechanism. In many cases the use of a combination of techniques, such as scintillators with proportional counters[17-19], have been used to obtain better data and

to verify conclusions drawn from the experiment.

The detector used in the present investigation is a gridded ionization chamber. Such a device has been used with considerable efficacy by other workers in the determination of nuclear reaction cross sections. Bellamy and Flack[20] studied the $^{40}Ar(n,\alpha)^{37}S$ reaction at 14 Mev, using a gridded ionization chamber filled to 30 atmospheres argon, and identified five alpha groups corresponding to five levels in ^{37}S. More recently, the same reaction was studied by Davis et al[21] in the energy range from 1.2 to 9.0 Mev. They used a gridded ionization chamber filled to various pressures between 2 and 9 atmospheres of argon and reported energy levels in ^{37}S which corresponded in most respects to those reported by Bellamy and Flack. The values of the cross section reported by Bellamy and Flack differed markedly from the values predicted by extrapolation of the results of Davis' group. Davis and colleagues at Rice University also used the gridded ionization chamber to study the (n,α) and (n,p) reactions on ^{14}N(Ref. 22), ^{10}B and ^{19}F(Ref. 23), and ^{16}O and ^{12}C(Ref. 24).

The purpose of the present investigation is to study the reactions of ^{20}Ne, ^{40}Ar and other nuclides with 14 Mev neutrons, leading to the emission of charged particles such as alphas, protons and tritons. These data provide information about the energy levels of reaction products and the cross

sections to the various energy states. The gridded ionization chamber does not permit measurement of differential cross sections or angular correlations.

II. APPARATUS AND PROCEDURES

Preliminary experiments showed that ordinary gas flow proportional counters were inadequate for high resolution alpha spectroscopy. These small proportional counters exhibited large non-reproducible errors attributable to wall effects and very poor resolution. Solid state detectors suffer the disadvantage of their components having high (n,p) cross sections which would lead to tremendous backgrounds (e.g. $\sigma_{(n,p)}$ for ^{28}Si is 250 mb at 14.5 MeV). Therefor a large volume gridded ionization chamber was obtained from Argonne National Laboratory.

The advantage of a gridded type ionization chamber over an ordinary ionization chamber is that the height of the output pulse does not depend on the position or orientation of the charged particle track. Figure 1 is a schematic diagram of a classic type Frisch grid chamber[25] used for solid samples. A grid is located between the two electrodes and maintained at an appropriate intermediate potential. The collecting electrode is positive relative to the other electrodes. The sample, emitting either alpha particles or other short range radiation is placed on the grounded electrode.

The grid shields the collecting electrode from the positively charged particles that are emitted between the grid and the grounded electrode. Since the positive ions remain in this region they induce no positive charge on the collecting electrode. In this way only the electrons

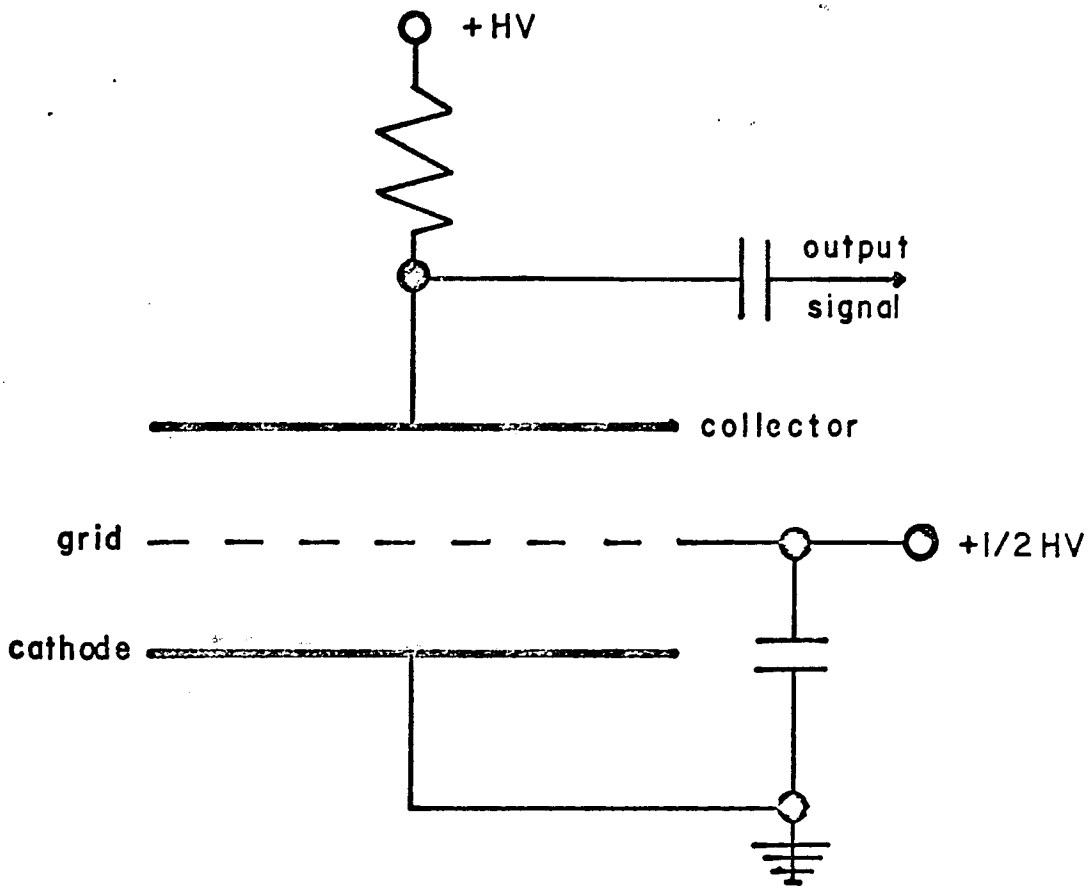

Figure 1.

Schematic of Frisch Type Gridded Ionization chamber.

produced by ionization will be collected. It is theoretically possible to adjust conditions so that no electron will be captured by the positive grid[26,27]. Thus the charge appearing at the collector will be equal to the total ionization produced by the charged particle in the sensitive volume.

The ANL chamber (Figure 2) has a sensitive volume of approximately two liters. It consists of an outer case, a series of rings to which potential is applied to collimate the charged particles and electrons, a grid, and a collection anode. In operation, the anode and case are at ground potential while the first ring, A-1, is at a negative potential, usually 3500 volts. The potentials on the other rings are controlled by a resistor chain which goes to ground potential at the anode guard ring, A-6. The grid, G, is also in the resistor chain and is at a potential equal to half that on A-1. Since slight variations may occur over a period of time in the very large resistors that constitute the chain, the potential of the grid could be different than exactly half the potential of A-1. In order to correct for such drift, G is maintained at the proper potential by a separate input from the same power supply that controls A-1. The power supply, a Power Designs model HV-1545, has two outputs, one of which has been modified to be at one half the potential of the other. The anode is ground with respect to A-1, but is not earth grounded, so that it collects the charge of the electrons which reach its surface.

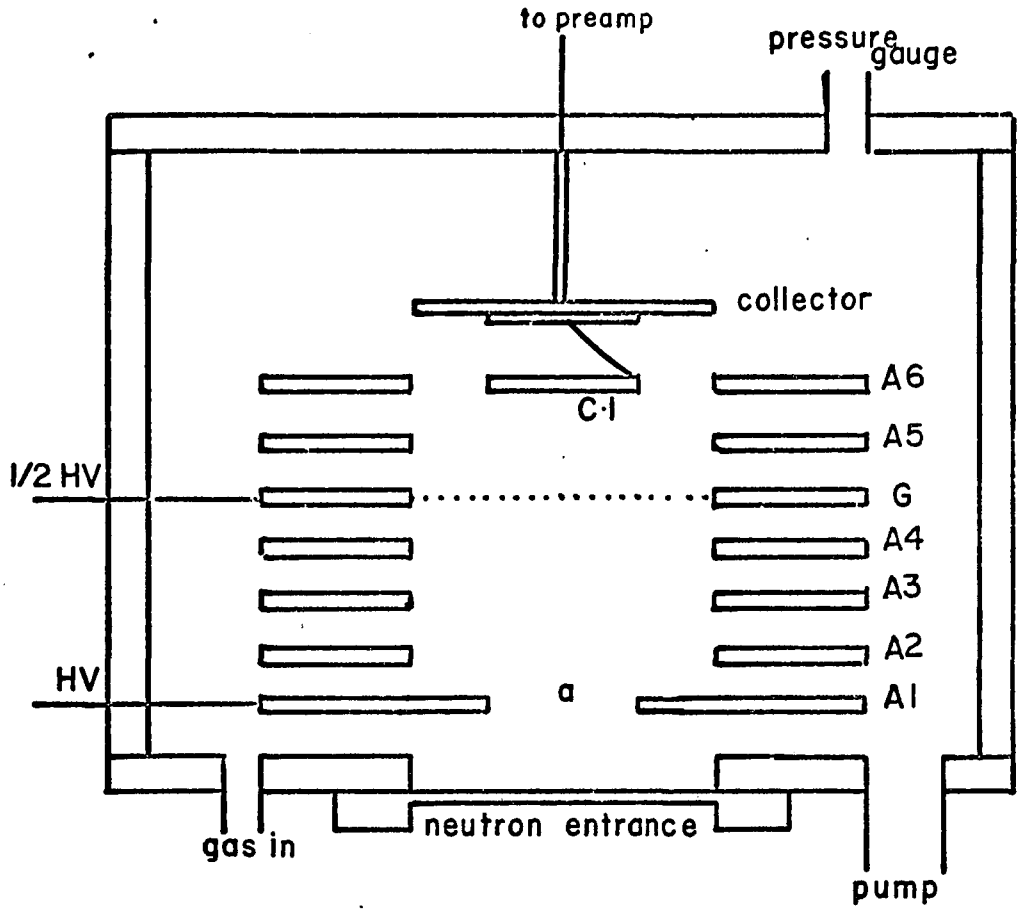

Figure 2.

Schematic of ANL Gridded Ionization Chamber.

The ionization chamber was filled with the gas under study. The gases (methane, neon-methane, and argon-methane mixtures) were purified by passing through molecular sieves maintained at liquid nitrogen temperature. The methane used was Matheson "Technical Grade" which is 97.0% pure. Oxygen and carbon dioxide, which are the impurities most detrimental to pulse height resolution, were present to the extent of 0.2% and 0.3% respectively. Both these impurities are readily removed by the purification method used. The neon used was Matheson "Purified Grade" which has a 99.7% minimum purity. P-10 counting gas (90% argon, 10% methane) was used for the argon methane mixtures.

Neutrons of approximately 14.3 MeV were obtained by the d(t,n) reaction in a Technical Measurement Corporation Activatron III neutron generator. The neutron flux was monitored with Teflon discs utilizing the $^{19}F(n,2n)^{18}F$ reaction. The product nucleus, ^{18}F, has a half life of 110 minutes and gives rise to 0.511 Mev annhilation radiation. A 3" x 4" NaI(Tl) detector, in fixed geometry, was used to detect the gamma radiation. The associated electronics consisted of a Chase preamplifier, Cosmic model 901AP amplifier, Cosmic model 801 single channel analyzer and a RIDL model 49-25 scaler-timer. The absolute counting rate was determined by comparison with a ^{22}Na standard which had been calibrated by the γ-γ coincidence method. The efficay of Teflon discs for neutron flux monitors has been demonstrated by Priest, Burns and Priest[28], and Shiokawa et al[29].

In practice, five Teflon discs of approximately 0.8 cm diameter and 0.1 cm thickness were placed on the exterior side of the neutron entrance to the ionization chamber (Figure 2) and then counted upon completion of the irradiation. The discs, which had been pre-weighed, were reusable since essentially all the ^{18}F activity disappears after ten half lives (1100 minutes). A correlation was made between the neutron flux at the neutron entrance and inside the chamber by making an irradiation with five discs at the neutron entrance and five discs at position "a" in the chamber (figure 2). It was found that the flux at the exterior position was 4.5 ± 25% greater than at position "a". Also, at position "a" the flux was distributed uniformly over the area covered by Teflon discs while in the exterior position there was as much as a 300% difference in the flux over the area tested. This was due to the proximity of the exterior foils to the target which led to great variations in the solid angle each subtanded.

The charge pulse generated in the ion chamber by the neutron induced reactions was shaped by a Canberra model 1406 charge sensitive preamplifier. The preamplifier output was futher amplified by an Ortec model 440 selectable filter amplifier and an Ortec model 408 biased amplifier. The pulses were then analyzed by a RIDL model 30-12B 400 channel analyzer and recorded by an IBM typewriter print out. The electronics were tested and calibrated with an Ortec model 419 test pulse generator.

The characteristics of the entire system was studied with an ^{241}Am source placed at position "a" in the chamber. The alpha spectrum obtained from the ^{241}Am is shown in figure 3. Under ideal conditions the resolution obtained was better than 1 percent at 5.48 MeV. Under actual experimental conditions compromises were made which adversely affected the resolution.

There are a number of factors inherent in the experimental procedure which distort the pulse height spectra and therefore influence the pulse height resolution. These factors are: (1) electron attachment, (2) columnar recombination, (3) nuclear reactions occuring outside the sensitive volume, (4) electronic noise and (5) wall effects.

Electron attachment is the phenomenon in which primary electrons become attached to neutral gas molecules before the former have been collected at the anode. The heavy negative ions so produced, migrate much more slowly than electrons in the collecting field and therefore will not contribute to the primary electron pulse in which they belong. Oxygen and water, the gases most responsible for electron attachment, are removed from the chamber fill by the method described previously. As a further precaution the chamber was baked out under vacuum in order to reduce the amount of oxygen and water adsorbed on the walls. It was found that when the same chamber fill was used for extended periods the resolution began to deteriorate. Consequently the chamber was periodically evacuated and refilled.

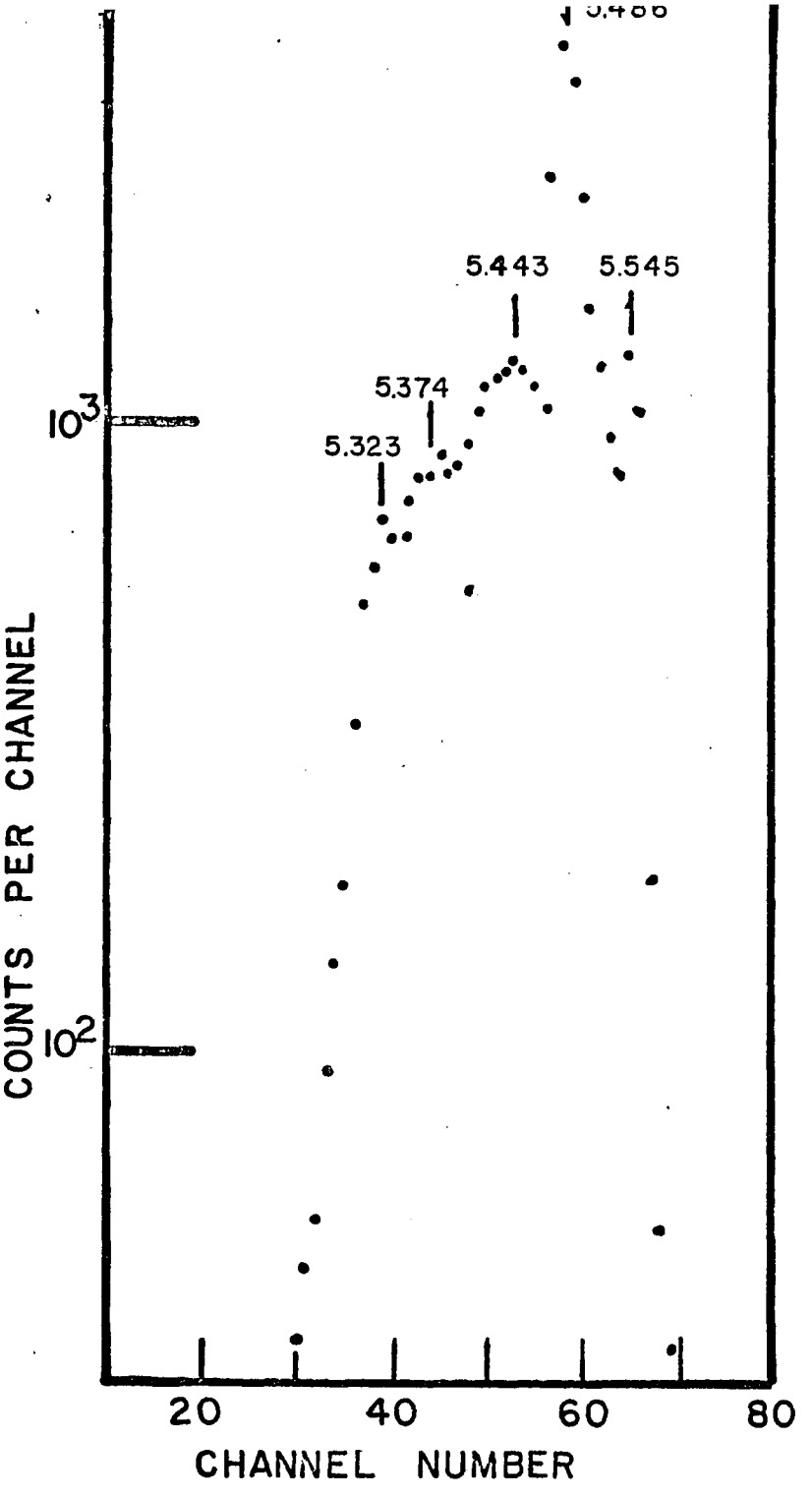

Figure 3.

Spectrum of Americium - 241.

Columnar recombination is the process in which positive ions and electrons recombine along the charged particle track. This effect increases with the density of ionization along the track and consequently is most significant at high pressures and for densely ionizing particles. The effect is not considered to be a serious problem at the pressures used in these experiments. Gabbard, Bischel and Bonner[22] reported a 10 percent peak broadening as pressure was increased from 3 to 7 atmospheres and a further 50 percent broadening from 7 to 10 atmospheres. In our experiments the pressure was maintained at approximately 2 atmospheres.

Nuclear reactions occur throughout the entire volume of the chamber since there is no way to confine the neutrons to the sensitive volume of the chamber. Disintegrations which occur between the grid and the collector give a continuous distribution in pulse size and contribute to the low energy side of the peaks. It was not possible to minimize this effect. Pulses caused by charged particles entering the sensitive volume after being formed by a reaction outside this region were eliminated by the insertion of a shield. The shield was a non-conducting cylinder of the dimensions of the sensitive volume. Charged particles produced in the region between the front chamber wall and A-1 (Figure 2) were prevented from entering the sensitive volume by a 0.005 cm aluminum foil fastened on the inner surface of A-1.

The primary source of electronic noise was the rf fields associated with the transformers that supply the high voltages to the neutron generator. The signal cable, which traverses a distance of fifty feet between the preamplifier, located in the neutron generator vault, and tha amplifier, at the generator console, passed directly over this noise producing area. This resulted in a noise spectrum consisting of several gaussian peaks. The peaks were intense and tended to drift up and down in energy rather abruptly. A noise cancellation circuit was constructed which consisted of a second cable, identical in electrical characteristics, wound in intimate contact with the signal cable. The second cable picked up the same rf signals as the primary cable and thus it was possible to cancel the noise in the signal cable at the amplifier inputs. There was no discernable electronic noise after elimination of the rf interferences. Electronic distortion of a test signal was found to be essentially nil.

The wall effect is a loss of events from the full energy peak due to charged particles which leave the sensitive volume of the chamber or strike the high voltage electrodes. Pulses corresponding to such tracks represent a loss in counts for which correction must be made in computing the areas under the peaks. The effect increases markedly with increasing path lengths. In order to determine the magnitude of the correction, a study of the

wall effect as a function of particle range in the chamber was performed. For track lengths short with respect to the dimensions of the sensitive volume the probability that a track will leave the sensitive volume is approximately[22]

$$\rho = \frac{r_o}{2}\left(\frac{1}{R} + \frac{1}{h_1}\right)$$

where r_o is the path length and R and h_1 are the radius and height of the sensitive volume respectivley. For ranges greater than 1.5 cm, the wall effect was studied by observing the effect of changes in pressure on the spectra from 5.48 MeV alpha particles of ^{241}Am and the alpha particles from the reaction $^{40}Ar(n,\alpha)$ to the ground state of ^{37}S. In the former case, the wall effect was studied, as a function of pressure from 0.25 to 2.0 atmospheres and in the latter from 1.0 to 5.0 atmospheres. For the $^{40}Ar(n,\alpha)$ experiments the results were normalized with respect to neutron flux and total number of ^{40}Ar nuclei. Theoretical aspects of wall effect calculations have been discussed by Hall[30] and by Snidow and Warren[31].

The results are shown in figure 4. In order to correct the value of the area under a particular peak the calculated integral is divided by the appropriate efficiency factor $(1-\rho)$. The range of an alpha particle of particular energy in the various gases used was obtained from the Bragg-Kleeman rule[32],

$$R_1 = \frac{3.2\times10^{-4}(A_1)^{\frac{1}{2}}}{Q_1} R_{air}$$

where R_1 is the range in a given gas and A_1 and Q_1 are

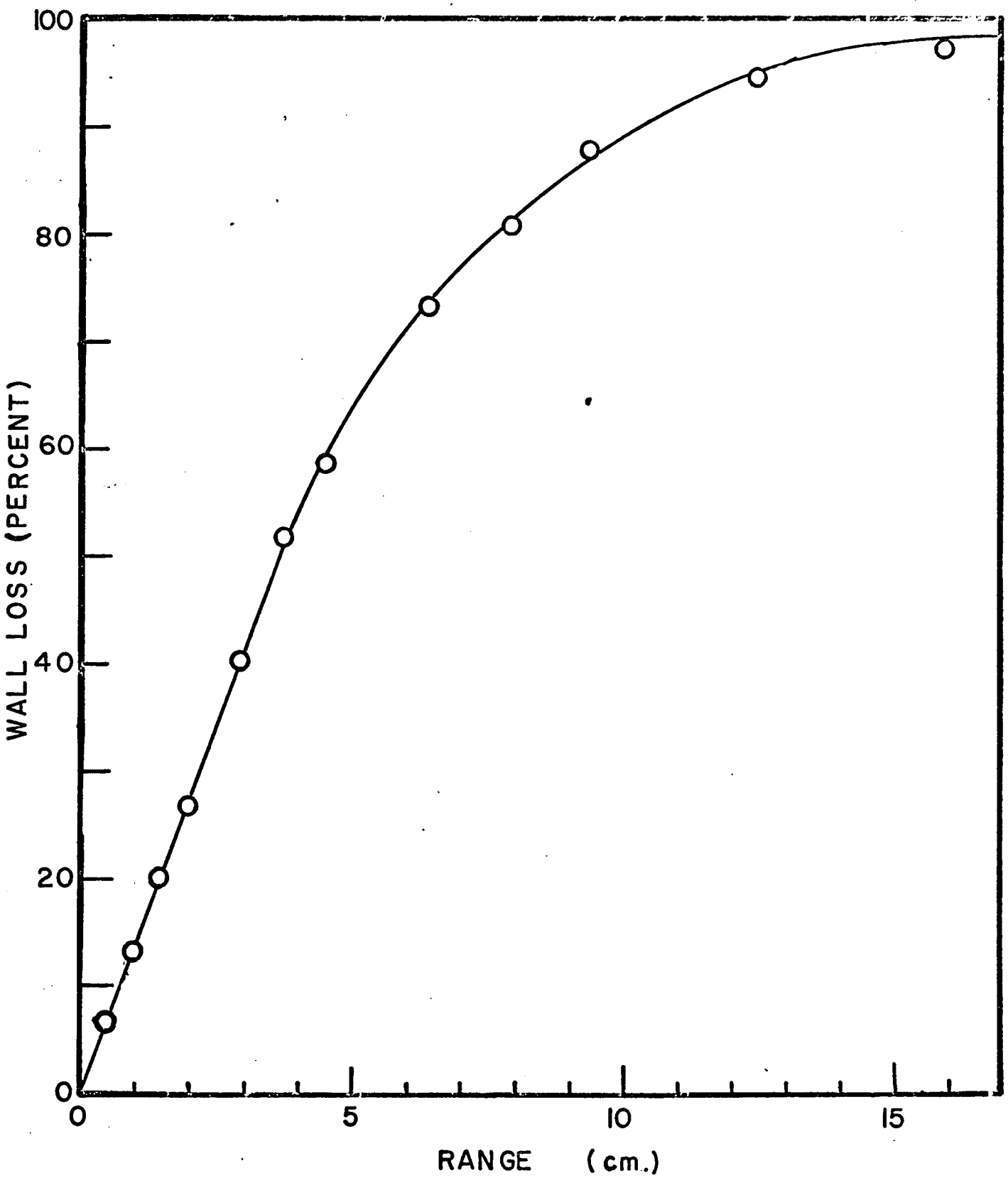

Figure 4.

Wall Loss as Function of Particle Range.

respectively the atomic weight and density of the gas. The values for the ranges of alpha particles in air, R_{air}, were taken from the tables of Jesse and Sadauskis[33]. These curves are shown in figures 5 and 6.

For a given nuclear reaction the number of events is given by the expression

$$R = n\sigma\Phi t \qquad (1)$$

where n is the number of target nuclei, σ is the cross section of the reaction in cm^2, Φ is the flux of incident particles and t is the time in seconds. R is obtained by measuring the areas under the appropriate peaks and correcting for wall losses and background; n can be obtained from the pressure, volume (sensitive) and temperature. The flux, Φ, is calculated from the Teflon disc monitors.

In order to obtain usable spectra it was necessary to operate at very low flux (approx. 10^6 $cm^{-2}sec^{-1}$, beam current 0.1 ma). At high fluxes, reactions with the components of the chamber itself yielded backgrounds which obscured the reactions under investigation. Operation at low flux however suffers the disadvantage of yielding low ^{18}F activities and consequently the value of the neutron flux is the least accurate term in equation (1). This limitation was surmounted by use of an internal flux monitor, namely the $^{12}C(n,\alpha_o)^9Be$ reaction.

For the determination of the $^{12}C(n,\alpha_o)$ cross section the ionization chamber is filled with pure methane. However,

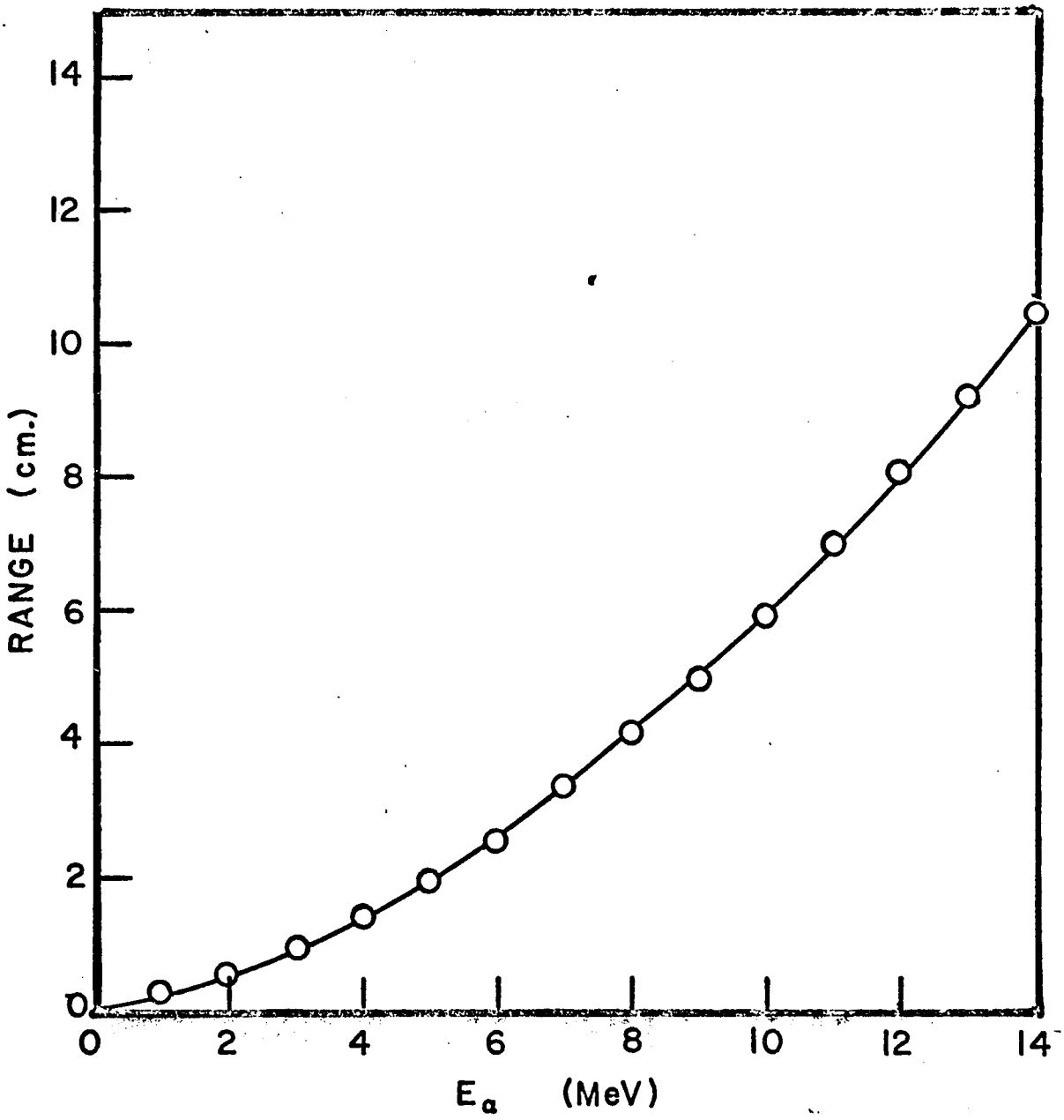

Figure 5.

Range of Alpha Particles in P-10 Gas as Function of Particle Energy.

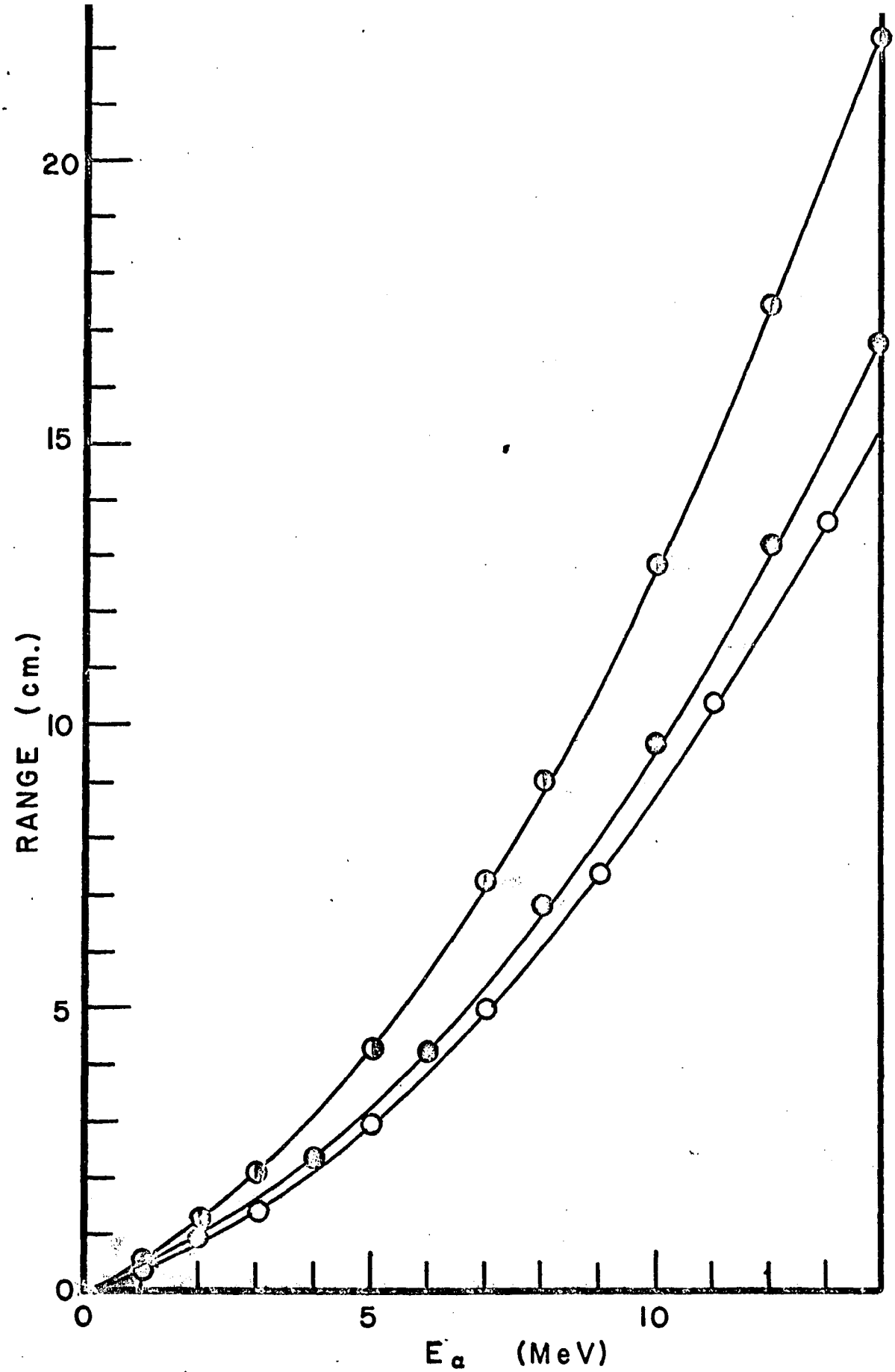

Figure 6.

Range of Alpha Particles in Various Neon-Methane Gas Mixtures as Function of Particle Energy.

in the experiments to measure (n,α) cross sections on ^{40}Ar and ^{20}Ne the pure gases are doped with a suitable quench gas which was, in both cases, methane. In these instances the $^{12}C(n,\alpha_o)$ reaction provided a convenient internal standard.

For two gases occupying the same volume the reactions induced on each can be obtained from equation (1), e.g. for methane and gas X

$$R_m = n_m \sigma_m \Phi t \qquad (2)$$

$$R_X = n_X \sigma_X \Phi t \ . \qquad (3)$$

Since both gases experience the same nutron flux and time of bombardment, dividing equation (2) into equation (3) gives

$$\frac{R_X}{R_m} = \frac{n_X \sigma_X}{n_m \sigma_m} \ . \qquad (4)$$

Assuming ideal behavior

$$\frac{n_X}{n_m} = \frac{P_X}{P_m} \qquad (5)$$

where P_X and P_m are the partial pressures of gas X and methane respectively. Substituting equation (5) into (4) and solving for σ_X yields

$$\sigma_X = \frac{R_X P_m}{R_m P_X} \cdot \sigma_m \ , \qquad (6)$$

where σ_m is a best value for the $^{12}C(n,\alpha_o)$ cross section at a particular energy. The values used for these experiments were 76 ± 11 mb and 69 ± 13 mb at 14.3 and 14.5 MeV respectively. The precision for these values surpassed those obtained for the Teflon disc flux monitors (approximately 35%). The

internal standard will be discussed in greater detail in a subsequent section.

Energy calibration of the spectra was accomplished via the 5.48 MeV alpha particle from the ^{241}Am standard and the $^{12}C(n,\alpha_o)$ peak, for which the Q-value is well known. As a check on the linearity of the spectrum the energy of the highest peak in the spectrum was calculated, on the assumption that it was a transition to the ground state, and compared with its theoretical Q-value. It was thus possible, utilizing these three peaks, to calculate the mean neutron energy as well as the energies of all the remaining peaks in the spectra.

III. RESULTS

a. Carbon-12

The spectrum obtained when methane is bombarded with neutrons having a mean energy of 14.3 MeV is shown in figure 7. The pulse distribution in channels 40 to 65 correspond to the 5.48 MeV alphas from the ^{241}Am standard. The pulses in channels 210 to 275 represent the alpha particles emitted in the $^{12}C(n,\alpha)$ reaction to the ground state of ^{9}Be. Alpha particles to excited states in ^{9}Be are not resolved although the end of the continuum at channel 160 may correspond to alpha transitions to the very broad state in ^{9}Be at 4.70 MeV. Resolution in this experiment was poor, about 16 percent.

The number of reactions, obtained by integration under the peak and correction for wall losses (70 percent), and the neutron flux calculated from the activity of the Teflon monitors gave a cross section of 75 ± 40 mb to the ground state of ^{9}Be.

b. Argon-40

Natural argon has three stable isotopes, ^{36}Ar, ^{38}Ar and ^{40}Ar with natural abundances of 0.337, 0.067 and 99.60 percent respectively[34]. Neutron induced reactions leading to emission of alpha particles, protons, deuterons and tritons are possible with all three isotopes at a neutron energy of 14.5 MeV. The Q-values for the respective reactions are[35,36];

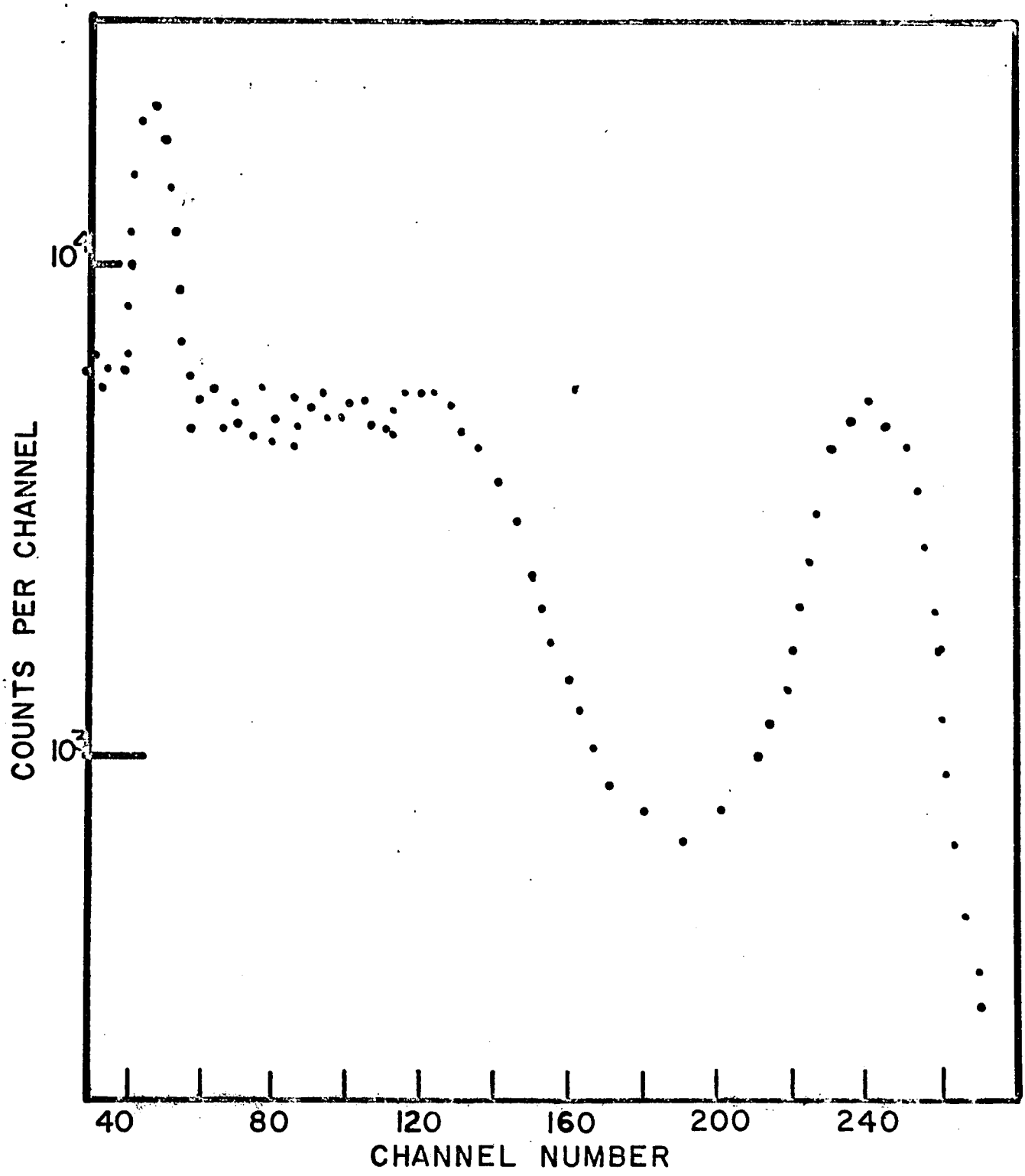

Figure 7.

Alpha Spectrum from Bombardment of Carbon-12.

$^{36}Ar + n \rightarrow {}^{33}S + \alpha$; Q = 2.00 MeV (1)

$\rightarrow {}^{36}Cl + p$; 0.07 MeV (2)

$\rightarrow {}^{35}Cl + d$; -10.30 MeV (3)

$\rightarrow {}^{34}Cl + t$; -12.72 Mev (4)

$^{38}Ar + n \rightarrow {}^{35}S + \alpha$; -0.23 MeV (5)

$\rightarrow {}^{38}Cl + p$; -4.13 MeV (6)

$\rightarrow {}^{37}Cl + d$; -8.03 MeV (7)

$\rightarrow {}^{36}Cl + t$; -12.09 MeV (8)

$^{40}Ar + n \rightarrow {}^{37}S + \alpha$; -2.41 MeV (9)

$\rightarrow {}^{40}Cl + p$; -6.76 MeV (10)

$\rightarrow {}^{39}Cl + d$; -10.30 Mev (11)

$\rightarrow {}^{38}Cl + t$; -12.11 MeV (12)

In the series of experiments on argon, pulses representing particle energies of less than 5.0 MeV were discriminated. Thus observation of reactions (3), (4), (7), (8), (11) and (12) was precluded.

A representative spectrum from the argon experiments is shown in figure 8. The peak in channels 140 to 172, with a mean energy of 8.75 MeV, corresponds to the $^{12}C(n,\alpha_o)$ reaction from the 10 percent methane present. The resolution for this pulse distribution is better than 4 percent, a marked improvement over the resolution when methane was the sole gas in the chamber. On the basis of the energy reference points provided by the 5.48 MeV alpha from ^{241}Am, at channel 23, and the $^{12}C(n,\alpha_0)$ reaction, the peak at channel 294 is calculated to have a mean energy of 12.04 MeV. This corresponds to a reaction having a Q-value of -2.41 MeV,

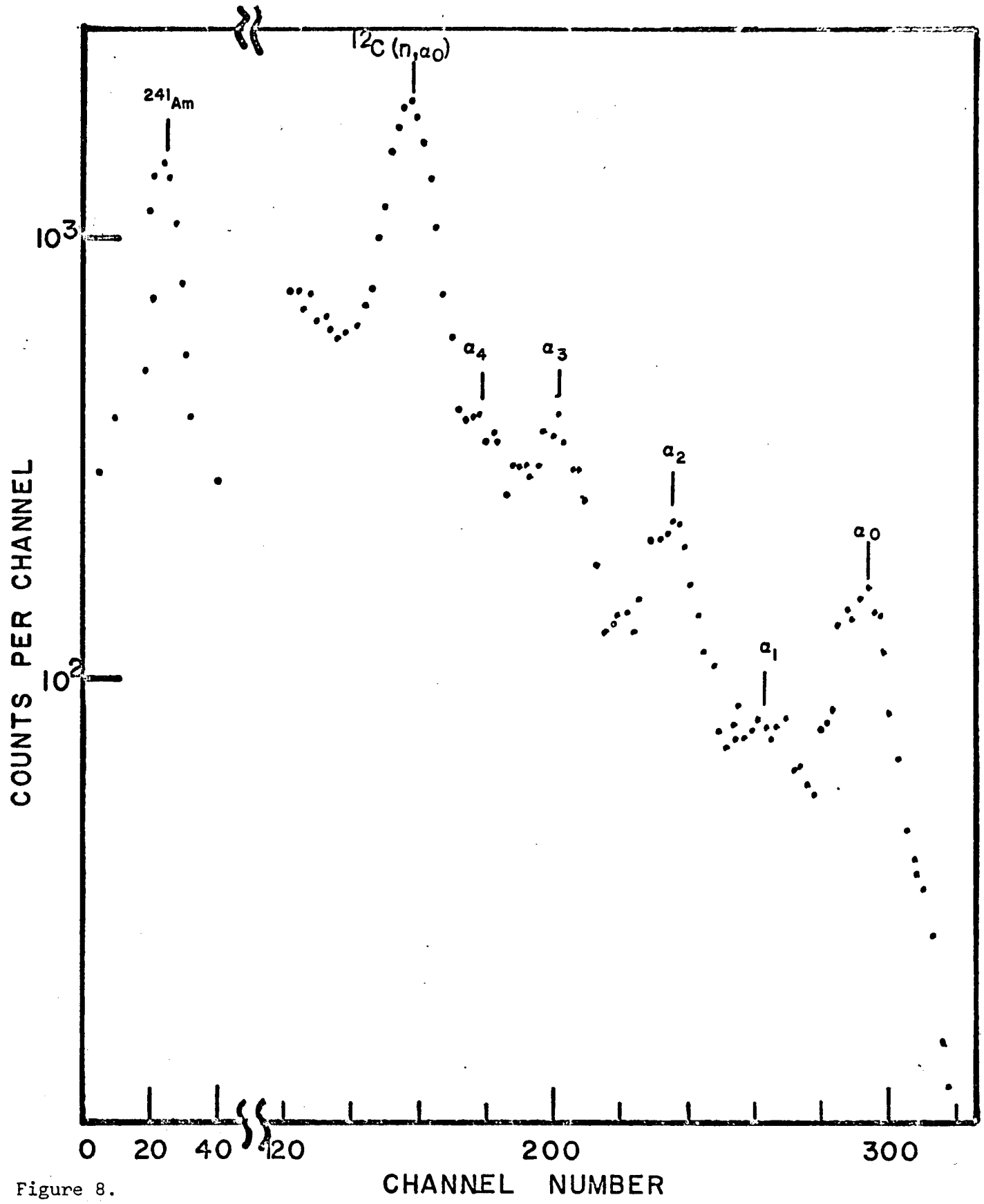

Figure 8.

Spectrum of Neutron Induced Reactions on Argon-40.

which can only be due to reaction (9), $^{40}Ar(n,\alpha)$ to the ground state of ^{37}S. The remaining peaks can all be assigned to the $^{40}Ar(n,\alpha)$ reaction to four excited states in ^{37}S. Although the peaks appearing in channels 203, 236 and 294 are intense and easy to assign, the assignment of energies to the less intense pulse height distributions in channels 178 and 265 were made only after careful analysis of the individual trials for this experiment. Evidence for these weak transitions was persistent in every experiment and could be attributed to no other causes. Resolution of the individual prominent peaks was, in all cases, better that 4 percent.

The data give the following energies for the first four excited states in ^{37}S; 0.59 ± 0.10 MeV, 1.39 ± 0.09 MeV, 2.20 ± 0.05 MeV and 2.83 ± 0.09 MeV. Indications of a peak corresponding to a level in ^{37}S at 3.50 ± 0.20 MeV were also observed in several experimental trials. No peaks could be discerned in the spectra which corresponded to reactions (1), (2), (5), (6) and (10).

The cross sections for the $^{40}Ar(n,\alpha)$ reactions were calculated using the $^{12}C(n,\alpha_0)$ cross section as reference. Variations in the values obtained for the cross sections to the levels in ^{37}S at 2.83 and 3.80 Mev from individual trials allowed only estimates to be made. The difficulties are due to poor statistics and higher backgrounds. Wall losses for the various peaks ranged from 61 percent for the alphas from the $^{12}C(n,\alpha_0)$ reaction to 81 percent for

the alphas from the $^{40}Ar(n,\alpha_0)$ reaction. The cross sections obtained are shown in table 1.

TABLE 1

14.45 MeV CROSS SECTIONS FOR ^{40}Ar*

Reaction	σ - mb	level in ^{37}S
$^{40}Ar(n,\alpha_0)$	2.1 ± 0.4	ground
(n,α_1)	0.3 ± 0.1	0.59 ± 0.10
(n,α_2)	3.1 ± 0.6	1.39 ± 0.09
(n,α_3)	3.5 ± 0.7	2.20 ± 0.05
(n,α_4)	≃ 0.3	2.83 ± 0.09
(n,α_5)	≃ 0.1	3.50 ± 0.20

*relative to $\sigma\ ^{12}C(n,\alpha_0) = 76 \pm 11$ mb

The total cross section for the $^{40}Ar(n,\alpha)^{37}S$ reaction can be estimated from the above to be; $\sigma \simeq 9.4 \pm 1.0$ mb. Since no other peaks could be observed in the spectra, it is unlikely that reactions to higher levels in ^{37}S, if such reactions exist, would contribute more than a negligible amount to the total cross section.

c. Neon-20

Naturally occuring neon consists of three stable isotopes; ^{20}Ne, ^{21}Ne and ^{22}Ne, which constitute 90.92, 0.26 and 8.82 percent of the total respectively[37]. The anticipated reactions for these nuclides with 14.5 MeV neutrons, and their respective Q-values are;

$^{20}Ne + n \rightarrow {}^{17}O + \alpha$; $Q = -0.59$ MeV (1)

$\rightarrow {}^{20}F + p$; -6.24 MeV (2)

$\rightarrow {}^{19}F + d$; -10.63 MeV (3)

$\rightarrow {}^{18}F + t$; -13.05 MeV (4)

$^{21}Ne + n \rightarrow {}^{18}O + \alpha$; -0.70 MeV (5)

$\rightarrow {}^{21}F + p$; -4.92 MeV (6)

$\rightarrow {}^{20}F + d$; -10.78 MeV (7)

$\rightarrow {}^{19}F + t$; -11.12 MeV (8)

$^{22}Ne + n \rightarrow {}^{19}O + \alpha$; -5.71 MeV (9)

$\rightarrow {}^{22}F + p$; -11.30 MeV (10)

$\rightarrow {}^{21}F + d$; -13.04 MeV (11)

$\rightarrow {}^{20}F + t$; -14.89 MeV (12)

The Q-values were obtained from published sources, if available[36], or calculated from nuclide mass tables[35].

The experiments with neon yielded the most complex spectra of all the gases studied. A typical spectrum is reproduced, in sections, in figures 9 and 10. The results from one experimental trial to the next exhibited excellent reproducibility. Examination of the different trials, however, led to the observation of weak transitions which appear more prominently in some spectra than in others. Thus the total number of reactions observed was greater than the number of peaks observed in any one experiment.

The energies of the individual peaks were determined in the manner previously described. In order to make energy level assignments with confidence the energies of the peaks

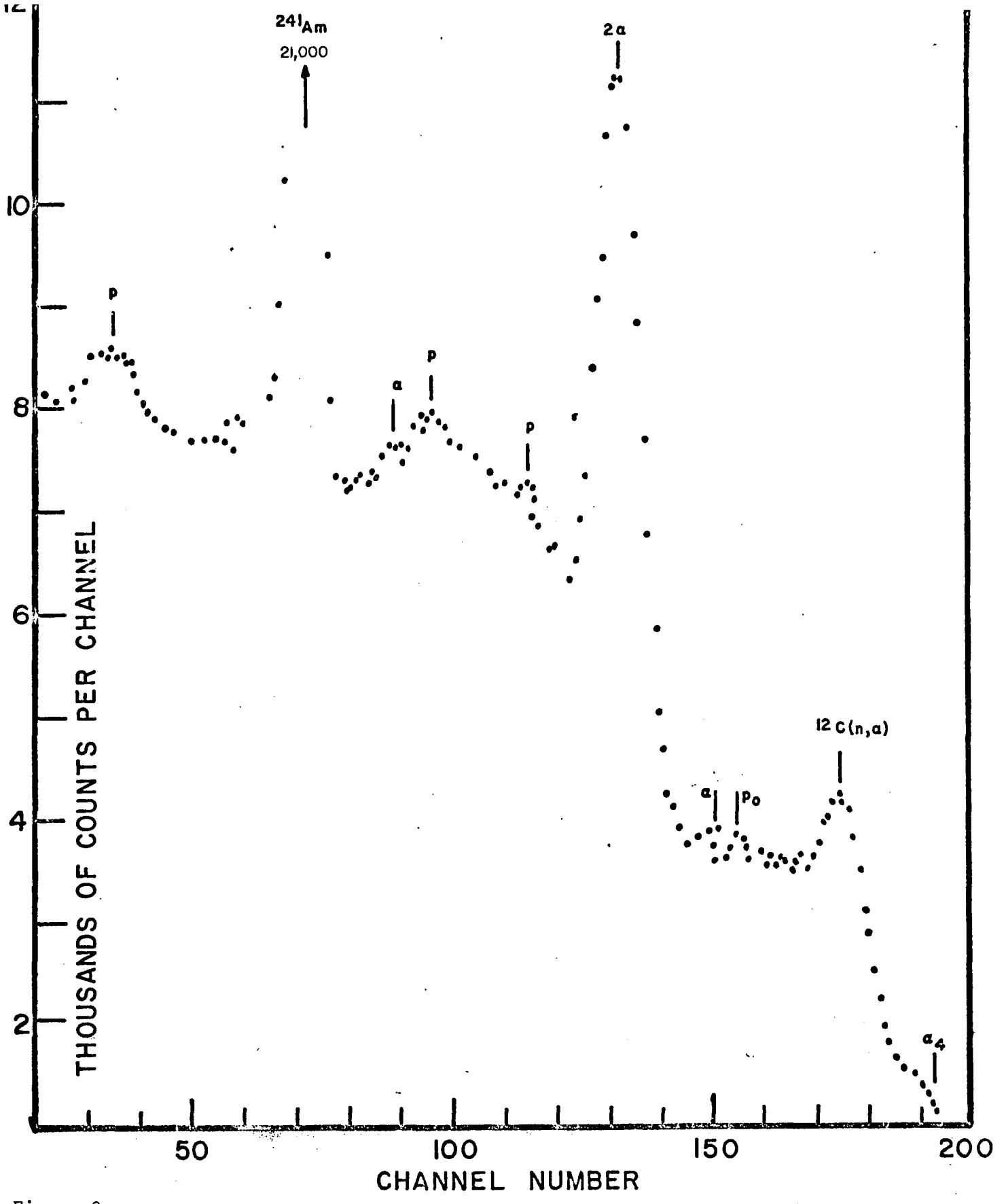

Figure 9.

Spectrum of Neutron Induced Reactions on Neon-20 (I)

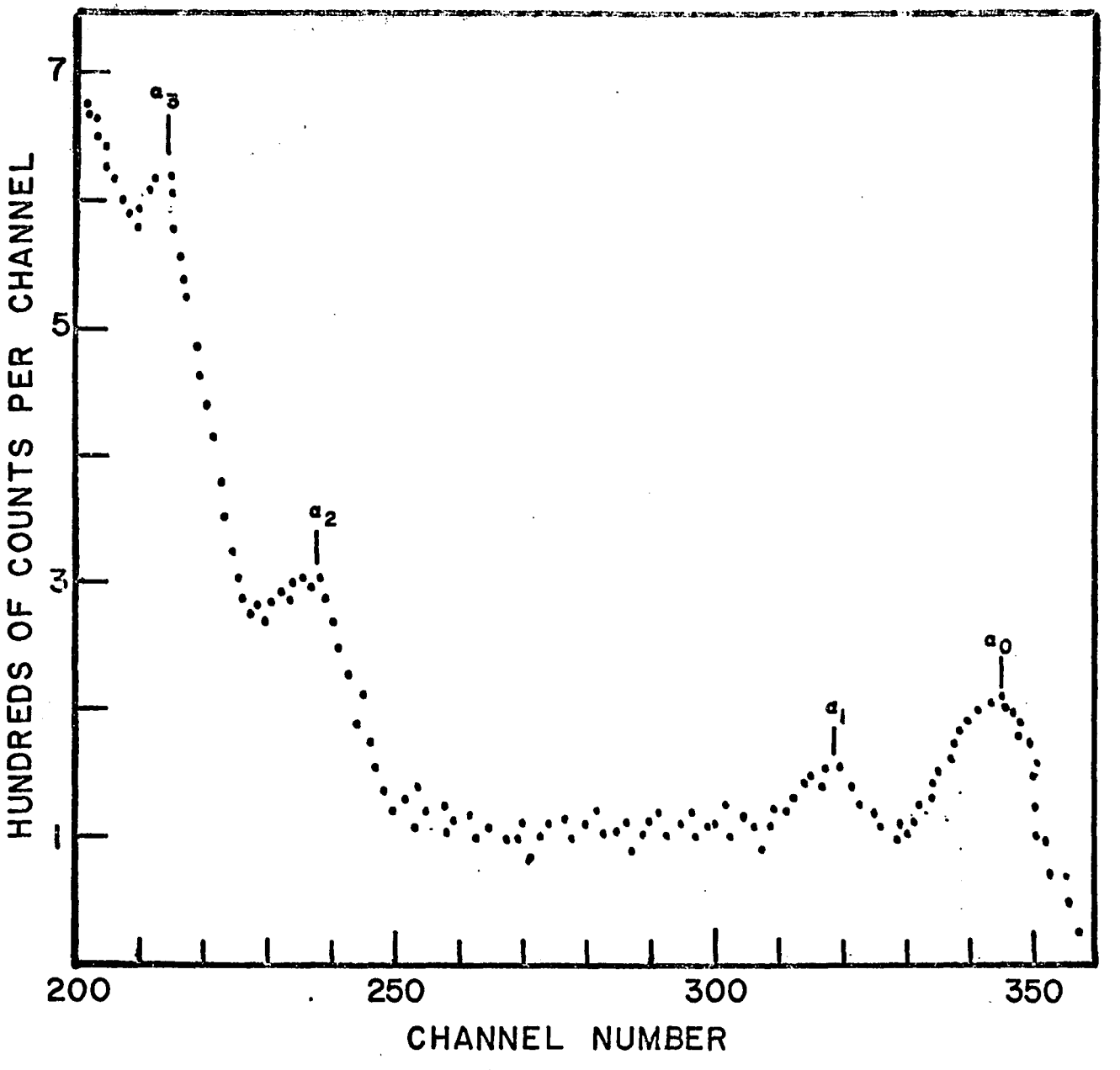

Figure 10.

Spectrum of Neutron Induced Reactions on Neon-20 (II)

were compared to theoretical Q-values and known energy level schemes,of the product nuclides, obtained from the literature. In this manner it was possible to arrive at peak assignments which were most consistent with the experimental data and with published information, As further evidence for peak assignments, the behavior of the peaks were studied as a function of target gas pressure in order to determine whether the transition was due to an alpha particle or a proton. This is possible since peak resolutions for alpha particles and protons change to different extents with increase, or decrease, in pressure. It has been shown[22] that the resolution of a peak due to an alpha particle is most rapidly deteriorated by an increase in pressure.

In the spectrum shown (figures 9, 10), the alpha particles from ^{241}Am and the $^{12}C(n,\alpha_0)$ reaction give peaks at channels 72 and 175 respectively. The peak at channel 346 is undoubtedly the alpha particle due to the $^{20}Ne(n,\alpha)$ reaction to the ground state of ^{17}O. The peaks in channels 188, 214, 239 and 320 correspond to the $^{20}Ne(n,\alpha)$ reaction to the first four excited states in ^{17}O. The peak in channel 149 also corresponds to a level in ^{17}O populated by the $^{20}Ne(n,\alpha)$ reaction. From this trial, and others, a total of eleven peaks due to the $^{20}Ne(n,\alpha)$ reaction were observed corresponding to transitions to the ground and ten excited states. The energy levels of ^{17}O calculated from these data are indicated in table 2.

TABLE 2

ENERGY LEVELS IN ^{17}O -MeV

0.83 ± 0.09
3.18 ± 0.12
3.90 ± 0.07
4.63 ± 0.12
5.55 ± 0.10
5.77 ± 0.15*
5.90 ± 0.10
7.22 ± 0.15*
7.61 ± 0.15*
7.77 ± 0.15*

An asterisk indicates those energy levels which were calculated from peaks observed in only one experimental trial, and thus must be considered as highly tentative.

The pulse distribution centered in channel 155 is identified as corresponding to protons from the $^{20}Ne(n,p)$ reaction to the ground state of ^{20}F. The same reaction, leading to the first excited state of ^{20}F, was detected in channel 115. The pulse distribution in the group of channels from 92 to 104 is due to a $^{20}Ne(n,p)$ reaction to another excited state in ^{20}F with some contribution from the $^{12}C(n,\alpha)$ reaction to the first excited state in ^{9}Be. The $^{12}C(n,\alpha)$ reaction to the broad 4.70 MeV state in ^{9}Be probably contributes the peak in channel 15.

As a result of the above experiments, levels in ^{20}F with energies of 1.23 ± 0.09, 1.80 ± 0.10, 2.9 ± 0.2 and 3.61 ± 0.10 MeV were observed. The level at 2.9 MeV is deduced from a persistent, but very weak, transition which accounts for the greater uncertainty in its value. The $^{20}Ne(n,p_o)$ peak yielded an experimental Q-value of -6.26 MeV for the $^{20}Ne(n,p)$ reaction. This is in excellent agreement with the predicted value of -6.24 MeV.

The most prominent peak in the spectrum is in channels 133 to 142. The intensity of the peak indicates that it is a transition to the ground state of some nuclide, but its Q-value, -7.00 ± 0.02 MeV, rules out all the reactions listed at the beginning of this section. A study of this peak as a function of methane concentration indicates that the peak is not due to reactions with ^{12}C. In addition, pressure studies show that the peak is due to alpha particles rather than protons. After consideration of many reactions which yield more than two products it was found that the Q-value for the reaction $^{20}Ne(n,2\alpha)^{13}C$ was very close to the experimentally derived Q-value. This reaction, with a theoretical Q-value of -6.95 MeV had been observed by Petralia et al, in a neon filled cloud chamber[16]. They were unable to calculate a Q-value due to poor statistics. However their data indicate the reaction to have a cross section at least an order of magnitude less than for the $^{20}Ne(n,\alpha_o)$ reaction. Our data, on the other hand, yielded

a cross section larger than that for $^{20}Ne(n,\alpha_0)$. This discrepancy will be discussed in a later section.

Resolution in the neon experiment was better than 5 percent on the $^{20}Ne(n,2\alpha)$ peak and 7 percent for the $^{20}Ne(n,\alpha)$ peak. The ^{241}Am standard exhibited a resolution of a little over 3 percent. The poorer resolution in the induced reaction peaks is due to chamber effects, as discussed earlier, and was expected.

Cross sections were calculated only for those reactions which gave reasonably reproducible results from one experiment to another. Wall losses for the neon experiment were high in the most energetic peaks. For example, the highest wall effect was 97 percent for the 13.94 MeV alpha particle from the $^{20}Ne(n,\alpha_0)$ reaction. For the reaction peaks with wall losses above 90 percent the largest single source of uncertainty in the cross section was the value of the wall loss correction $(1-\rho)$. The value for the $^{12}C(n,\alpha_0)$ cross section used as the standard was 69 ± 13 mb[38].

The experimentally determined cross sections for the various reactions in neon are listed in Table 3. In three instances values considered to be good estimates are also reported.

TABLE 3

14.3 MeV CROSS SECTIONS OF ^{20}Ne*

Reaction	σ - mb	
$^{20}Ne(n,\alpha_0)$	6.0 ± 2.4	to ground state ^{17}O
(n,α_1)	0.9 ± 0.4	to 0.83 MeV level ^{17}O
(n,α_2)	1.4 ± 0.4	to 3.18 MeV level ^{17}O
(n,α_3)	1.8 ± 0.4	to 3.90 MeV level ^{17}O
(n,α_4)	1.2 ± 0.3	to 4.63 MeV level ^{17}O
(n,α_5)	0.4†	to 5.55 MeV level ^{17}O
(n,α_7)	0.1†	to 5.90 MeV level ^{17}O
$(n,2\alpha)$	38.0 ± 7.6	to ground state ^{13}C
(n,p_0)	1†	to ground state ^{20}F

* relative to $\sigma\ ^{12}C(n,\ _0) = 69 \pm 13$ mb
† estimated

The total cross section for the $^{20}Ne(n,\alpha)^{17}O$ reaction was estimated from the above data to be $\geq$ 11.8 mb.

d. Precision and Accuracy

As indicated, resolution for the argon and neon experiments were excellent. This can be attributed to the design of the gridded ionization chamber and the state of the art electronics which were employed. Reproducibility was also quite good. For example, energy measurements used to establish the Q-value of the $^{20}Ne(n,2\alpha)$ reaction exhibited a precision of better than 0.3 percent. The precision for the $^{20}Ne(n,\alpha_0)$ reaction cross section was better than 10 percent and the results for the $^{20}Ne(n,2\alpha)$ reaction cross section were found to have a precision of better than 6 percent.

The primary sources of uncertainty in the values of the cross sections of reactions in argon and neon were;

(1) an error of ± 16 percent and ± 19 percent for argon and neon respectively due to the values of the $^{12}C(n,\alpha_o)$ cross section used as standards,

(2) the value of the wall effect correction which, in the extreme case, was estimated to be accurate to ± 25 percent.

Other sources of error, i.e. statistics of peak and background integration and determination of the partial pressures of the gases, contributed only slightly relative to the two major sources of error cited above.

The mean energy of the neutrons was determined for each individual experimental trial. This was performed by using the ^{241}Am, $^{12}C(n,\alpha_o)$ and the highest energy peak in the spectrum and calculating back to determine the neutron energy which would give the spectrum under consideration. The mean neutron energies were found to be 14.30 MeV and 14.45 MeV for the neon and argon experiments respectively. No reason could be found to account for a 150 KeV difference in neutron energy from one set of experiments to the other. However, assuming one value or the other to be incorrect, the variation in the reported results for energy levels and Q-values would still be within experimental error.

In addition to the experiments with methane, argon and neon, attempts were made to perform similar studies on nitrogen. Spectra obtained were very poor with essentially

no structure over background. This is somewhat surprising since Gabbard, Bischel and Bonner[22] used a gridded ionization chamber to study neutron induced reactions on nitrogen with good results. Since their study was concerned with neutron energies up to 9 MeV only, it is possible that at 14 MeV other mechanisms compete with direct (n,α) reactions which would complicate the spectra, e.g., inelastic scattering. The most probable explanation for our failure to obtain usable data is that the nitrogen was not sufficiently free of H_2O and O_2, even after passage through the cold trap, to prevent electron attachment.

IV. DISCUSSION

a. Carbon-12

The value determined for the $^{12}C(n,\alpha_o)$ cross section exhibited the largest experimental error of all the cross sections determined in this work. It is, however, interesting to compare our result with other work to illustrate the validity of our technique and also to justify use of the $^{12}C(n,\alpha_o)$ reaction as an internal standard. Table 4 lists the values of this cross section reported in the literature for neutron energies between 13.9 and 15.6 MeV.

TABLE 4

author	E_n - MeV	- mb
Brendle et al[38]	13.9	79 ± 20
Graves and Davis[39]	14.1	80 ± 20
Al-Kital and Peck[40]	14.1	62 ± 15
Kopsch and Cierjacks[41]	14.1	72.7 ± 6.8*
Kitazawa and Yamamuro[42]	14.1	76 ± 11
Chatterjee and Sen[43]	14.5	69 ± 13
Brendle et al[38]	15.6	77 ± 20
this work	14.3	75 ± 40

* the α_o transition is not accurately separated, at large angles α_o particles are lost.

Our result, despite its large uncertainty, agrees remarkably well with other work. It is seen that, within experimental error, the cross section for the $^{12}C(n,\alpha_o)$ reaction is more or less constant over the range of neutron

energies reported. The values used as standards in our calculations were those of Kitazawa and Yamamuro, for the neon, and Chatterjee and Sen, for argon. The difference in the cross section, calculated for various reactions in neon and argon, due to selection of one value of the $^{12}C(n,\alpha_o)$ cross section over another is no more than ± 10 percent. With the availability of more precise values for the $^{12}C(n,\alpha_o)$ cross section it would be possible to determine the cross sections of the neon and argon reaction with greater accuracy.

None of the listed literature values were obtained by the methods used for this paper. Most were done by either, nuclear emulsions[40,43], or scintillation techniques[38,42]. This does not mean that gridded ionization chambers are less applicable to this reaction than are other techniques. Redesign of the chamber (i.e. larger sensitive volume), and availability of ultrapure gas samples would certainly improve resolution and decrease wall effects. It should be possible, in future experiments, to resolve alpha particles to other levels in ^{9}Be. An interesting future experiment would be to look for the $^{12}C(n,n\alpha)^{8}Be$ reaction and the alpha particles from the subsequent break up of the ^{8}Be nucleus.

b. Argon-40

Energy levels in ^{37}S from the $^{40}Ar(n,\alpha)$ reaction have been reported by Bellamy and Flack[20] and Davis et al[21].

Both groups used apparatus similar to that used in our experiments but without benefit of recent advances in solid state electronics. Bellamy and Flack used neutrons of energies between 14.1 and 14.8 MeV but did not specify the exact energy from which their data was compiled. Davis et al studied the reactions in the range from 5.8 to 9.0 MeV.

TABLE 5

ENERGY LEVELS IN ^{37}S - MeV

This work	Bellamy and Flack	Davis et al
0.59 ± 0.10		0.65 ± 0.06
1.39 ± 0.09	1.3 ± 0.05	1.39 ± 0.07
2.20 ± 0.05	2.2 ± 0.1	2.19 ± 0.09
2.83 ± 0.09	2.7 ± 0.1	2.8 ± 0.2
3.5 ± 0.2	3.5 ± 0.2	

No other data is available for the level structure of ^{37}S. The 3090 keV gamma ray associated with ^{37}S(Refs. 44,45) is due to a transition in ^{37}Cl following the beta decay of ^{37}S.

As seen in table 5, Bellamy and Flack did not report the level in ^{37}S at 0.59 MeV. This was probably due to the low cross section of the $^{40}Ar(n,\alpha)^{37}S$ reaction at 14 MeV and the very high background exhibited in their spectra. Davis et al had no difficulty with this peak since at 9 MeV its cross section is about three times greater than its value at 14 MeV. On the other hand, Davis et al did not report the 3.5 MeV level. Most likely this was due to a

high conentration of nitrogen impurity in the argon which led to a prominent recoil peak at the lower end of their spectrum. This recoil peak apparently obscured the 3.5 MeV level. Our data is otherwise in excellent agreement with that of both groups of experimenters.

The only data available for the cross sections of $^{40}Ar(n,\alpha)$ reactions to various levels in ^{37}S, at 14 Mev neutron energy, is from the work of Bellamy and Flack. They report a cross section to the ground state of 30 ± 15 μb which is almost two orders of magnitude less than the value of 2.1 ± 0.4 mb reported here. The great discrepancy may be due, in part, to the fact that they calculated neutron flux, indirectly, from the integrated deuteron flux incident on the tritium target. Also, they did not mention wall effects at all in their paper, leaving one to assume that they may not have taken this effect into account.

Although they do not calculate other cross sections, Bellamy and Flack do give relative intensities of their peaks as 1.0/1.45/2.2/1.15/1 for the transitions to the ground and second through fourth excited states. This trend is in general agreement with our cross section values of 2.1 ± 0.4, 3.1 ± 0.6 and 3.5 ± 0.7 mb which correspond to the first three peaks they observed (they do not report the 0.59 MeV level).

Table 6 lists previously reported values of the $^{40}Ar(n,\alpha)$ total cross sections and two semiemperical

predictions. Our value for this cross section is also included in the table.

TABLE 6

TOTAL CROSS SECTIONS FOR $^{40}Ar(n,\alpha)^{37}S$

author	E_n - MeV	σ - mb
Ranakumar et al[45]	14.4	10.5 ± 1.0
Husain and Kuroda[46]	14.4	10 ± 1.5
Mathur and Morgan[14]	14.1	13 ± 1.5
	14.1	2*
	14.5	3*
Gray et al[47]	14.5	24 ± 2
Yu and Gardner[48]	14.1	31 ± 5†
Gardner and Yu[49]	14.1	30.2¶
this work	14.5	9.4 ± 1.0

* theoretical prediction, based on compound nucleus theory and statistical model for decay of compound nucleus.
† experimental value; error does not include uncertainty in reaction used for standard.
¶ theoretical prediction, semiemperical; based on statistical model.

Our experimental value for the total $^{40}Ar(n,\alpha)$ cross section is in excellent agreement with the most recent of the values listed in the table. These cross sections, due to Ranakumar et al and Husain and Kuroda, were both determined by activation techniques. Our result is also in good agreement with that of Mathur and Morgan who used a scintillation counter to observe the prompt alpha particles emitted. They also used standard activation techniques on

liquid argon samples. The experimental values of Gray et al and Yu and Gardner are not consistent with the previously discussed results.

Our results do not confirm either of the theoretical predictions listed in the table. Indeed, all indications are that the reaction proceeds via a direct mechanism which would minimize the significance of the predictions of Mathur and Morgan based on compound nucleus theory. Although the experimental value reported by Gardner and Yu seems to confirm their own prediction, based on a statistical model, both values, predicted and experimental, are inconsistent with the other experimentally derived values.

c. Neon-20

The nuclear level structure of ^{17}O has been studied extensively by various researchers. Reactions such as $^{13}C(\alpha,\alpha')$ (Ref. 50), $^{13}C(\alpha,n)$ (Ref. 50), $^{16}O(d,p)$ (Ref. 51), $^{16}O(n,n')$ (Ref. 52) and $^{15}N(d,\alpha)$ (Ref. 53) have been employed to obtain ^{17}O as either a compound nuclear state or as end product in a direct reaction. Table 7 lists the energy levels of ^{17}O obtained from a recent compilation[54] and from a more recent determination of higher energy levels[52]. Our values are compared with those obtained from the literature.

TABLE 7

ENERGY LEVELS IN ^{17}O - MeV

this work	literature
0.83 ± 0.09	0.871
4.18 ± 0.12	3.06
3.90 ± 0.07	3.85
4.63 ± 0.12	4.55
5.55 ± 0.10	5.38/5.70
5.77 ± 0.15	5.73
5.90 ± 0.10	5.89
7.22 ± 0.15	7.24
7.61 ± 0.15	7.69
7.77 ± 0.15	7.70/7.83

All the values reported in this work agree with the literature within experimental error. In the cases of the levels we report at 5.55 and 7.77 MeV it is difficult to know which of the two literature values listed for each corresponds most closely. It is possible that each of the peaks from which the levels at 5.55 and 7.77 MeV were determined were actually combinations of two or more transitions to closely lying levels. We did not see other levels which have been reported in the literature in our spectra. This may be due to very low cross sections for the $^{20}Ne(n,\alpha)$ reaction to these levels or, excessively large backgrounds in the appropriate regions of the spectrum. For example, the $^{20}Ne(n,2\alpha)$ peak would certainly

obscure any transitions to levels reported in the literature between 6.24 and 6.37 MeV.

The energy levels of ^{20}F have also been extensively studied and reported[55-59]. As in the case of ^{17}O and ^{37}S the values for ^{20}F levels in the literature were determined by means other than the method utilized here. The four levels herein deduced correspond, within experimental error, to levels reported in the literature. Again, many levels reported by other workers are not observed, due to low cross sections and high backgrounds.

Only one value for the $^{20}Ne(n,\alpha)$ cross section is reported in the literature. McDicken and Jack[60] studied the angular distributions of the alpha particles to the ground and first excited states of ^{17}O and concluded that a direct mechanism, such as pick up, was taking place. Their angular distributions disagree with those of Cevolani et al [15] who concluded that heavy particle stripping was a primary mechanism. McDicken and Jack report values of 5.5 ± 0.9 and 4.0 ± 0.6 mb for the cross sections to the ground and 0.871 MeV levels of ^{17}O respectively. Our value of 6.0 ± 2.4 mb is in good agreement with theirs for the ground state transition, however our value of 0.9 ± 0.4 mb for the cross section to the 0.871 MeV level disagrees with theirs by a factor of about four.

It is difficult to see, from their paper, how McDicken and Jack can claim values for the cross sections of the

$^{20}Ne(n,\alpha)$ reactions determined to ± 15 percent. Indeed from their own spectrum, the error due to counting statistics alone is of the order of ± 25 percent. Also, each peak is determined by only four or five points, compounding the possibility of even greater uncertainties. In addition to the above McDicken and Jack claim an error of ± 5 percent in neutron flux determination while they do not actually measure flux at the reaction target chamber. Flux measurement was carried out by proton recoil monitors placed at positions assumed to be equivilant to the position of the reaction chamber. In retrospect, it would seem that a value of the $^{20}Ne(n,\alpha)$ cross section to ± 40 or 50 percent would be more realistic in the McDicken and Jack paper.

McDicken and Jack state that they could not obtain statistically accurate data at large backward angles. It is at these large backward angles, however, where the contribution to the angular distribution that Cevolani et al report, in their paper, would be found. Despite their admitted difficulties McDicken and Jack base their disagreement with Cevolani et al on the differences between the angular distributions at large backward angles. The possibility that heavy particle stripping plays an increasingly major role in transitions to higher energy levels would help to resolve the differences, real or imagined, between the two groups. Indeed Cevolanis' data

indicates support for this conclusion.

The $^{20}Ne(n,2\alpha)^{13}C$ reaction, as indicated, was reported by Petralia et al[16] who are colleagues of Cevolani. Both papers were based on data obtained in the same experiment. Although Petralia does not report a Q-value for the reaction his data would seem to give support for the value of Q obtained by us, -7.00 ± 0.02 MeV. This value is also in good agreement with the value calculated from the mass tables. Their are four possible mechanisms for the $^{20}Ne(n,2\alpha)$ reaction which correspond to a theoretical Q-value of -6.95 MeV.

$$^{20}Ne + n \rightarrow {}^{13}C + {}^{8}Be^{*}$$
$$\downarrow$$
$$^{8}Be^{*} \rightarrow 2\alpha \qquad (1)$$

$$\rightarrow {}^{13}C + 2\alpha \qquad (2)$$

$$\rightarrow \alpha + {}^{17}O^{*}$$
$$\downarrow$$
$$^{17}O^{*} \rightarrow {}^{13}C + \alpha \qquad (3)$$

$$\rightarrow {}^{21}Ne^{*} \rightarrow {}^{13}C + 2\alpha \qquad (4)$$

Mechanisms (3) and (4) both proceed via some compound nucleus although (3) is partially a direct reaction. In both cases the ^{13}C nucleus and at least one alpha particle should be emitted isotropically. Petralia et al have shown that the angular distribution of the alpha particle is peaked strongly at large backward angles, indicating that heavy particle stripping is a factor. This data minimizes the significance of mechanisms (3) and (4).

Petralias' data seems to indicate that the cross section

for the $^{20}Ne(n,2\alpha)$ reaction is an order of magnitude less than that for $^{20}Ne(n,\alpha)$. This is in opposition to our results which show the $^{20}Ne(n,2\alpha)$ cross section to be greater than for $^{20}Ne(n,\alpha)$. It is difficult to see how such a discrepancy could be resolved. The possibility is suggested, however, that since Petralia studied only three pronged events, in the cloud chamber, he may have missed any $^{20}Ne(n,2\alpha)$ reactions which would proceed via a series of two pronged reactions such as in (1), (3) and (4). The fact that our spectra show the $^{20}Ne(n,\alpha)$ reaction to proceed via a direct reaction (the spacings between the $^{20}Ne(n,\alpha)$ alpha particle energies correspond to levels in ^{17}O rather than in ^{21}Ne) makes it unlikely that reactions through the ^{21}Ne compound nucleus are significant for the $^{20}Ne(n,2\alpha)$ reaction at 14 MeV. This would eliminate, as does Petralias' data, reaction (4).

Of the remaining reactions, (1) is a two step process and (2) is a direct one step mechanism. If the possibility that the reaction does proceed partly through a one step, three prong, reaction and partly via reaction (1) is valid, we can estimate, on the basis of our cross section and Petralias' relative two prong/three prong reaction ratio, the percentage of reactions which go by one of the two mechanisms. This estimate would show the $^{20}Ne(n,2\alpha)$ direct reaction proceeds via mechanism (1) 90 percent of the time and via mechanism (2) 10 percent. This conclusion is based

on an ad hoc hypothesis and must await independent confirmation which is not presently available. An attempt to provide additional data to this problem by analyzing the relative resolutions of the (n,α) and $(n,2\alpha)$ peaks was inconclusive.

d. General comments

Although other researchers have used gridded ionization chambers to study nuclear reactions we believe this set of experiments to be the most significant above neutron energies of 9 MeV. The techniques used have enabled us to deduce energy levels of several nuclei and to calculate cross sections to these various energy levels. In most cases where prior data exists, agreement is excellent.

We believe the use of an internal standard as a flux monitor to be of significance in this series of experiments. The use of the $^{12}C(n,\alpha_o)$ reaction obviated the use of independent monitors for determination of neutron flux and greatly simplified calculations.More precise determination of the $^{12}C(n,\alpha_o)$ reaction cross section over a wide range of neutron energies will make the use of this internal standard an even more powerful tool. In cases where the α_o peak from the $^{12}C(n,\alpha_o)$ reaction might interfere with other data, selection of another reaction as internal standard should be possible.

Experiments of a similar nature to the work reported here should be performed. In order to improve results, a chamber of greater sensitive volume might be constructed.

This would decrease the losses due to wall effects. Whether or not a larger chamber is constructed, the great backgrounds could be reduced by coating the electrodes and collection plate with approximately 0.025 cm of gold metal. The gold coating would essentially eliminate (n,p) reactions on these surfaces which contribute a great amount of the background in the higher energy channels. Use of a recently purchased 4096 channel analyzer would also simplify interpretation of the data. In order for the relationship derived in section II to be valid all data must be taken in one run. It was found that 400 channels often restricted the observable energy range since at higher amplifier gain all the data needed could not fit in the analyzer memory; i.e. in order to keep the ^{241}Am peak and the peak due to the highest energy alpha particle in 400 channels it was necessary to compress the spectrum making resolution of neighboring peaks difficult.

Future experiments with gases would be greatly simplified if isotopically enriched gases were used. In the case of neon, for example, background and peaks from reactions on ^{20}Ne obscured all trace of any reactions on ^{21}Ne and ^{22}Ne. By varying the isotopic ratios from trial to trial, peaks could be more definitely assigned to reactions of one nuclide or another. The possibility of using gaseous organo-metallic compounds should also be considered.

One of the first experiments undertaken, in laying the groundwork for this dissertation, was a unsuccessful attempt

to use metal foils as targets on position "a" in the chamber (Figure 2). Because of the large backgrounds due to nuclear reactions with the chamber fill it was not possible to detect reactions occuring with the metal foil. Selection of an appropriate counting gas mixture may solve this problem. A possible gas mixture might contain helium as the major component if a way is found to prevent the electrical breakdown that occurs in helium at elevated potentials.

As indicated, the work reported by no means exhausts the possible studies that can be made using thse techniques. Additional equipment, such as a linear accelerator, Van deGraff or variable energy cyclotron, would widen the scope of potential research even more. In any event the use of the gridded ionization chamber to study in-situ reactions has been shown to supply useful data. Much interesting work remains to be performed.

APPENDIX

Sample Cross Section Calculation For $^{20}Ne(n,2\alpha)^{13}C$

$$\sigma x = \frac{P_m(1-\rho_m)R_x}{P_x(1-\rho_x)R_m} gm$$

	expt'l value	error	error type
P_m	205 torr	± 1%	systematic
P_x	1164 torr	± 1%	systematic
$1-\rho_m$	0.22	± 10%	systematic
$1-\rho_x$	0.23	± 10%	systematic
R_x	25,543 counts	± 346 counts	statistical
R_m	7,279 counts	± 233 counts	statistical
σ_m	69.0 mb	± 13.0 mb	systematic

$$\sigma_x = 38.9 \pm 8.2 \text{ mb}$$

BIBLIOGRAPHY

1. M.A. Preston, "Physics of the Nucleus" Addison Weley, (1962)
2. J.M. Blatt and V.F. Weisskopf, "Theoretical Nuclear Physics" Wiley (1952)
3. J.R. Oppenheimer and M. Phillips, Phys. Rev. 48 (1935) 500
4. E.O. Lawrence, E. McMillan and R.L. Thornton, Phys. Rev. 48 (1935) 493
5. S.T. Butler, Phys. Rev. 80 (1950) 1095
6. S.T. Butler, Nature 166 (1950) 709
7. S.T. Butler, Proc. Roy. Soc. (London) 208A (1951) 559
8. O.N. Kaul, Nucl. Phys. 33 (1962) 177
9. N. Cindro et al, Nucl. Phys. 22 (1961) 96
10. B. LeRoux et al, Nucl. Phys. 67 (1965) 333
11. D. Schwalm and B. Povh, Nucl. Phys. 89 (1966) 401
12. R. Bachinger and M. Uhl, Nucl. Phys. A116 (1968) 673
13. B. LeRoux et al, Nucl. Phys. A116 (1968) 196
14. S.C. Mathur and I.L. Morgan, Nucl. Phys. 75 (1965) 561
15. M. Cevolani, G. DiCapariacco and S. Petralia, Nucl. Phys. 79 (1966) 379
16. S. Petralia et al, Nouvo Cimento 44 (1966) 225
17. D.R. Maxson and R.D. Murphy, Nucl. Phys. A110 (1968) 555
18. D.R. Maxson, R.D. Murphy and M.R. Zatzick, Nucl. Phys. A110 (1968) 609

19. M. Fazio et al, Nucl. Phys. A111 (1968) 255

20. E.H. Bellamy and F.C. Flack, Phil. Mag. 46 (1955) 341

21. E.A. Davis et al, Nucl. Phys. 55 (1964) 643

22. F. Gabbard, H. Bischel and T.W. Bonner, Nucl. Phys. 14 (1959/60) 277

23. E.A. Davis et al,Nucl. Phys. 27 (1961) 448

24. E.A. Davis et al, Nucl. Phys. 48 (1963) 169

25. O.R. Frisch, British Atomic Energy Rept. Br-49 (1944)

26. O. Bunemann, NRC Report PD-285 (1946)

27. O. Bunemann, T.E. Cranshaw and J.A. Harvey, Can.J. Phys. A27 (1949) 191

28. H.F. Priest, F.C. Burns and G.L. Priest, Nucl. Instrum. Meth. 50 (1967) 141

29. T. Shiokawa et al, J. Inorg. Nucl. Chem., 30 (1968) 1

30. G. Hall, Nucl. Instr. 3 (1961) 121

31. N.L. Snidow and H.D. Warren, Technical Paper, TP-305; Babcock and Wilcox Nuclear Development Center (1966)

32. G. Knop and W. Paul, "Interaction of Electrons and Alpha Particles with Matter"; Chapter I of "Alpha, Beta and Gamma Ray Spectroscopy" K. Siegbahn, Ed. North Holland (1966)

33. W.P. Jesse and J. Sadauskis, Phys. Rev. 78 (1950) 1

34. A.O. Nier, Phys. Rev. 77 (1950) 789

35. M. Hillman, "An Extended Table of Nuclidic Masses" BNL 846 (1964)

36. S.C. Mathur, J.B. Ashe and I.L. Morgan, "Compilation of Neutron Reaction and Total Cross Sections at 14 MeV"; Texas Nuclear Corp., Austin. (1963)

37. W. Seelmann-Eggebert et al,"Chart of the Nuclides" Third Edition; Karlsruhe. (1968)

38. M. Brendle et al, Z. Naturforschung. 23 (1968) 1229

39. E.R. Graves and R.W. Davis, Phys, Rev. 97 (1955) 1205

40. R.A. Al-Kital and R.A. Peck Jr., Phys. Rev. 130 (1963) 1500

41. D. Kopsch and S. Cierjacks, Nucl. Instrum. Meth. 54 (1967) 277

42. H. Kitazawa and N. Yamamuro, J. Phys. Soc. Japan. 26 (1969) 600

43. M.L. Chatterjee and B. Sen, Nucl. Phys. 51 (1964) 583

44. S. Wirjoamidjojo and B.D. Kern, Phys. Rev. 163 (1967) 1094

45. N. Ranakumar, E. Kartunnen and R.W. Fink, Nucl. Phys. A128 (1969) 333

46. L. Husain and P. Kuroda, J. Inorg. Nucl. Chem. 30 (1968) 355

47. P.R. Gray, A.R. Zander and T.G. Ebrey, Nucl. Phys. 62 (1965) 172

48. Yu-Wen Yu and D.G. Gardner, Nucl. Phys. A98 (1967) 451

49. D.G. Gardner and Yu-Wen Yu, Nucl. Phys. 60 (1964) 59

50. B.K. Barnes, T.A. Belote and J.R. Risser, Phys. Rev. 140 (1965) B616

51. R.E. McDonald et al, (Conf-650410-42)

52. D. Lister and A. Sayres, Phys. Rev. 143 (1966) 745

53. Y.I. Titov, A.P. Klyucharev and V.D. Vynirailenko, Yadern Fiz. 4 (1966) 308

54. C.M. Lederer, J.M. Hollander and I. Pearlman, "Table of the Isotopes" Sixth Ed., Wiley (1967)

55. T. Lauritsen and F. Ajzenberg-Selove, Nucl Phys. 11 (1959) 1

56. G. Goldhaber, Phys. Rev. Lett. 4 (1960) 1

57. V.M. Rout et al, Nucl. Phys. 45 (1963) 369

58. T.R. Shagnon, Nucl. Phys. 59 (1964) 257

59. R.W. Newsome, Nucl. Phys. 71 (1965) 353

60. W.N. McDicken and W. Jack, Nucl. Phys. 88 (1966) 457

ABSTRACT

NUCLEAR REACTIONS OF ^{12}C, ^{20}Ne and ^{40}Ar INDUCED BY 14 MeV NEUTRONS

by

STANLEY KARDONSKY

Advisors: Dr. H.L. Finston
Dr. E.T. Williams

A gridded ionization chamber was used to study neutron induced reactions, in-situ, of ^{12}C, ^{20}Ne and ^{40}Ar. Cross sections were calculated for these reactions to various energy levels in the product nuclei, utilizing the $^{12}C(n, \alpha_0)^9Be$ reaction as a neutron flux standard.

The cross section for the $^{12}C(n, \alpha_0)$ reaction was found to be 75 ± 40 mb. The $^{40}Ar(n, \alpha)$ reaction total cross section was 9.4 ± 1.0 mb. Cross sections of the $^{20}Ne(n,p_0)$ and $^{20}Ne(n,2\alpha)$ reactions were measured; these values were 1 mb and 38.0 ± 7.6 mb respectively. The total cross section of the $^{20}Ne(n, \alpha)$ reaction was measured to be 11.8 mb.

Energy levels in product nucleus ^{37}S at 0.59 ± 0.10 MeV, 1.39 ± 0.09 MeV, 2.20 ± 0.05 MeV, 2.83 ± 0.09 MeV and 3.50 ± 0.20 MeV were observed and found to be in excellent agreement with previously reported values. Ten levels in product nucleus ^{17}O were observed and found in agreement with prior work.

Experimental cross sections, herein reported, for ^{40}Ar

and ^{20}Ne were compared with theoretical and semiemperical predictions. The data indicated that all the above reactions proceed via direct mechanisms. A hypothesis as to the mechanism of the $^{20}Ne(n,2\alpha)$ reaction is presented which suggests the reaction proceeds via two competing mechanisms.

AUTOBIOGRAPHICAL SKETCH

Stanley Kardonsky was born in Brooklyn, New York on November 21, 1941. He attended the New York City public school system including Brooklyn Technical High School at which he majored in chemistry. In 1963 he received the degree of Bachelor of Science in Chemistry from Long Island University. In the following year he was awarded a Masters degree from the University of Florida, at which he majored in chemical physics.

In December, 1961 he married Elaine Wasserman. From this union has come two children; Stacey, born in Florida in 1963, and Mark Henry in 1965